SUPPLEMENTAL INFORMATION

The tumor suppressor folliculin regulates AMPK-dependent metabolic transformation

Ming Yan, Marie-Claude Gingras, Elaine A. Dunlop, Yann Nouët, Fanny Dupuy, Zahra Jalali, Elite Possik, Barry J. Coull, Dmitri Kharitidi, Anders Bondo Dydensborg, Brandon Faubert, Miriam Kamps, Sylvie Sabourin, Rachael S. Preston, David Mark Davies, Taren Roughead, Laëtitia Chotard, Maurice A.M. van Steensel, Russell Jones, Andrew R. Tee, and Arnim Pause.

Supplemental methods

Plasmids, Antibodies and biochemical reagents

The SV40LT-pMSCV and Cre-Neo-pMSCV vectors were kind gifts from Dr. N. Sonenberg (McGill University, Montreal, Canada). The mouse-*Flcn*-pMSCV vector was a gift from Dr. M.C. Simon (University of Pennsylvania, Philadelphia, USA) and the *Flcn* cDNA was subcloned into a 2XFlag-MigR1 retroviral vector. The 2XFlag was first inserted into MigR1 vector by restriction using BglI and EcoR1 sites and then the mouse *Flcn* cDNA was subcloned into EcoR1 site. The mutation of FLCN serine 62 to alanine (S62A) was generated with the Quick Change Site-Directed Mutagenesis kit (Stratagene) according to the manufacturer's instructions, using the *Flcn*-pMSCV construct as template and modified S62A forward and reverse primers (sequence are detailed in Supplemental Table S3). The human-*Flcn* cDNA was obtained from Dr. L.S. Schmidt (NCI, Bethesda, MD, USA) and was subcloned into a 2xFlag-pcDNA3 vector (1). The anti-mouse FLCN polyclonal antibody was generated by the McGill animal resource center services through injecting purified GST-FLCN recombinant protein in rabbits. The β-actin (AC74; Sigma-Aldrich), HIF-1α (Cayman Chemical Company), HIF-2α (Abcam), Flag (M2; Sigma-Aldrich), PGC-1α (4C1.3; Calbiochem), tubulin (T9026; Sigma), FNIP1 (Novus Biologicals), AMPKα (2532; Cell Signaling Technology), phospho (Thr172) AMPKα (2531; Cell Signaling Technology), ACC (3676; Cell Signaling Technology) and phospho (S79) ACC

(3661; Cell Signaling Technology) antibodies are commercially available. The antibodies used for immunohistochemistry staining were HIF-1α (NB100-123; Novus Biologicals), MTC02 Mitochondrial Marker (AB3298), BNIP3 (AB38621 Abcam), GLUT1 (AB652; Abcam) and VEGF-A (sc-152 Santa Cruz Biotechnology) and are commercially available. The N-acetyl cysteine (NAC) was purchased from Sigma-Aldrich.

Cell culture

Primary MEFs were isolated from E12.5 *Flcn* floxed mice (generously gifted by Dr. L.S. Schmidt, NCI, Bethesda, MD, USA) and cultured by standard methods (2). *Flcn* wild-type (WT) and knockout (KO) MEFs were generated after immortalization of primary *Flcn*$^{Flox/Flox}$ MEFs with SV40 large T (hygromycin B) and retroviral infection with a CD8 or CD8-Cre recombinase construct, followed by flow cytometry cell sorting of CD8 positive cells. The FLCN rescued knockout cells (Resc) were generated by retroviral infection with 2X-Flag-Flcn-MigR1 (puromycin) wild type (WT), S62A mutant or empty vector (EV) constructs. *Ampk*$^{+/+}$ and *Ampk*$^{-/-}$ MEFs have been described in (3) and UOK257 (FLCN-) / UOK257-2 (FLCN+) cells were kindly gifted by Dr. L.S. Schmidt (NCI, Bethesda, MD, USA) (4). The human follicular thyroid cancer cell line FTC-133 cells naturally deficient for FLCN were obtained from Dr. E.R. Maher (University of Birmingham, Birmingham, UK) and were previously described in (5, 6). FTC-133 cell were stably rescued for FLCN expression using 2XFlag-pcDNA3 human FLCN construct or an empty vector as control. MEFs, UOK257 and UOK257-2 were maintained in Dulbecco's modified Eagle's medium (DMEM), and FTC-133 cells were maintained in 50:50 DMEM:F12 media. Cell culture medium was supplemented with 10% (v/v) fetal bovine serum (FBS), 100 U/ml penicillin and 100μg/ml streptomycin (Invitrogen). UOK257-2 cell medium was

supplemented with 5ug/ml blasticidin S and rescued MEFs and FTC-133 with G418 (0.5 mg/ml) to maintain FLCN expression. MEFs and FTC-133 cells stably downregulated for FLCN, HIF-1α or PGC-1α expression were generated using the Mission lentivirus shRNA empty vector (shEV), a scrambled sequence (shScram2; Sigma-Aldrich), FLCN knockdown (shFlcn) (purchased from Sigma-Aldrich), PGC-1α knockdown (shPGC-1α) (generously gifted by Dr. S. Huang, McGill University, Montreal, Canada) or two HIF-1α (shHIF) specific sequences targeting mouse or human. HIF-1α shRNA-A was obtained from Dr. R.G. Jones (McGill University, Montreal, Canada) and described in (3) and targeted mouse and human sequence, while two independent shRNA targeting mouse or human HIF-1α were purchased from Sigma-Aldrich (shHIF-1α B).

Cell Proliferation and Survival assays

MEFs were seeded (2×10^4 cells) in 12-well plates in triplicate and 100μM glucose or glutamine free medium was added 24 h after plating. Cell numbers were counted daily using Coulter Counter (Beckman) and proliferation and survival rates were determined as the fold or percent cell number compared to day 0, respectively.

Quantification of mitochondria content by genomic qPCR

Total cellular DNA was extracted from UOK257 or MEFs using the DNeasy Blood and Tissue Kit (Qiagen). Relative nuclear (human RPL13A or mouse β-globin) and mitochondrial (human cytochrome B or mouse Cox2) DNA levels were quantified by qPCR (sequences are detailed in Supplementary table S3) and results were expressed as the percent mitochondrial DNA normalized to the nuclear DNA content (% mtDNA/nDNA).

RNA Extraction, quantitative PCR (qPCR) and real time PCR (qRT-PCR)

Total RNA was extracted using the RNeasy mini kit (Qiagen) and reverse-transcribed using the Superscript III kit (Invitrogen). Quantitative real-time PCR (qRT-PCR) was performed using Express SYBR Green qPCR supermix (Invitrogen) and specific primers (sequences are detailed in Supplemental table S3). Dissociation curves confirmed single product amplification and results were normalized to housekeeping genes 18S or RPLP0 (sequences are detailed in Supplemental table S3).

Protein extraction, immunoprecipitation and western blotting

Cells were washed twice with cold phosphate-buffered saline (PBS), lysed in AMPK lysis buffer (7), supplemented with Complete protease inhibitor (Roche) and DTT (1 mM), and cell lysates were cleared by centrifugation at 13000*xg*. For immunoprecipitation, cleared lysates were incubated with the EZview Red anti-Flag M2 beads (Sigma-Aldrich) for 2 h at 4°C. Beads were washed 3 times with lysis buffer and Flag-FLCN complexes were eluted twice with 150ng/ml of Flag peptides diluted in PBS. For cell lysates, cells were washed twice with cold PBS and lysed directly in Laemmli buffer (62.5 mM Tris-HCL (pH 6.8), 2% (w/v) sodium dodecyl sulphate, 10% (v/v) glycerol, 5% (v/v) β-mercaptoethanol and 0.01% (w/v) bromophenol blue). Proteins were separated on SDS-PAGE gels and revealed by western blot as we previously described (8) using the antibodies listed above.

Soft agar and xenograft assays

Two-layered soft agar assays were undertaken in six-well plates. Briefly, subconfluent FTC-133 or UOK257 cells (3×10^5) were plated in complete media supplemented with TSH (10U/L),

containing 0,35% agar over a 0,6% agar layer. Agar was overlaid with complete media and colonies were grown for 14 to 21 days at 37°C in 5% CO_2. Media were changed twice a week. Cell colonies were then stained with crystal violet (0.0005%) and representative pictures were taken using inverted CKX41 microscope (Olympus) equipped with an Infinity camera (Luminera Corporation). For xenograft assays, 5 x 10^6 FTC-133 cells resuspended in 200µL of PBS were injected subcutaneously into the flank of nude mice. Tumor length (l) and width (w) were measured twice a week using a caliper and the tumor volume (V) was calculated ($V = 1/2(l \times w^2)$).

Immunohistochemistry

Procedures have been described in details previously (8). Briefly, sections of formalin-fixed paraffin-embedded (FFPE) kidney tumor sample and normal controls were deparaffinized in xylene and dehydrated through graded ethanol concentrations. Endogenous peroxidase activity was blocked by incubation in 3 % (w/v) hydrogen peroxide (H_2O_2) in methanol for 30 min, followed by microwave treatment using 10mM citrate buffer (pH 6) for 10 min (90W) for MTC02, BNIP3, GLUT1 and VEGF-A and using 20mM TE buffer (pH 9) for HIF-1α to facilitate antigen retrieval. Sections were incubated with primary antibodies in 3% (w/v) bovine serum albumin overnight at 5ºC. Slides were washed 3 times with PBS and secondary antibody (EnVision, DAKO) was applied for 30 min at room temperature. Slides were washed 3 times with H_2O_2, revealed using DAB solution (EnVision, Dako), counterstained haematoxylin and embedded in Entellan (Electron Microscopy Sciences).

Supplemental legends:

Supplementary Figure S1: **Increase mitochondrial biogenesis in FLCN deficient human kidney cancer cells and ROS-dependent activation of HIF upon loss of FLCN in MEFs under hypoxia.** A) Percent mitochondrial DNA content (mtDNA) normalized to nuclear DNA content (nDNA) measured in the indicated MEFs and the FLCN-deficient UOK257 (EV) and FLCN rescued (Resc) human kidney cancer cells. B) Fold ROS levels measured in the indicated UOK257 cells. C) Relative HIF activity measured under hypoxia using HIF-luciferase reporter assay in *Flcn* knockout MEFs, rescued (Resc) or not (KO) for FLCN expression and treated with the indicated concentrations of the anti-oxidant, N-acetyl cysteine (NAC) for 16 h. Data represent the means ± SD of 3 independent experiments performed in triplicate. *$p < 0.05$, **$p < 0.01$, ***$p < 0.001$.

Supplementary Figure S2: PGC-1 upregulation upon loss of FLCN in human kidney cancer cells. Relative PPARGC1A and PPARGC1B mRNA expression levels measured in FLCN-deficient (EV) and FLCN rescued (WT) human kidney UOK257 cancer cells. Data represent the means ± SD of five independent experiments performed in triplicate. **$p < 0.01$.

Supplementary Figure S3: **Loss of FLCN in MEF does not affect cell proliferation.** *Flcn* WT and KO MEFs proliferation rate were determined by cell counting in time course experiments. Data represent the mean ± SD of six independent experiments performed in triplicate.

Supplementary Figure S4: HIF-dependent metabolic advantage drives tumorigenesis in FLCN null cancer cells. A, C) Western blot analysis of FLCN and HIF-1α expression levels in

the indicated FTC-133 (A) and UOK257 (C) cancer cell lines. Actin was shown as loading control. When indicated, cells were pretreated with Dimethyloxaloylglycine (DMOG), an inhibitor of HIF-1α prolyl hydroxylases that prevent HIF-1α degradation. Results are representative of 3 independent experiments. B) Representative pictures of soft agar colonies in the indicated FTC-133 cell lines. Scale bar: 500μM. D) Quantification of soft agar colonies number relative to FLCN-deficient UOK257 cells rescued for FLCN expression (KO + Resc). Data represent the means ± SD of 4 independent experiments performed in triplicate. E) Time course measurement of xenograft tumor volume in the indicated FTC-133 cell lines. n= 5 mice per group.

Supplemental tables:

Table S1: Fold metabolites levels measured in MEFs

Pathway	Metabolites	WT		KO		*p*-value	N
		MEAN	SD	MEAN	SD		
glycolysis	Glucose	1,0	0,2	1,4	0,2	0,00002	8
	F6/G6P	1,0	0,1	1,4	0,5	0,01398	8
	F1,6bisP	1,0	0,2	1,6	0,9	0,01621	8
	DHAP/G3P	1,0	0,4	1,5	0,4	0,00979	8
	3PGA	1,0	0,3	1,5	0,4	0,00454	8
	R5P/RL5P	1,0	0,4	1,6	0,3	0,01189	8
	pSer	1,0	0,4	1,6	0,8	0,01614	8
	Ser	1,0	0,2	1,4	0,2	0,00253	8
	Ala	1,0	0,2	1,6	0,4	0,00001	8
TCA cycle	Glutamine	1,0	0,2	1,4	0,4	0,01101	8
	Fumarate	1,0	0,1	1,4	0,2	0,00165	8
	Succinate	1,0	0,1	1,5	0,4	0,00445	8
	Citrate	1,0	0,1	1,4	0,2	0,00055	8
	α-ketoglutarate	1,0	0,2	1,7	0,6	0,01260	8

Table S2: Fold metabolites levels derived from Glucose or Glutamine labelled source

Flux	Metabolites		WT		KO		*p*-value	N
			MEAN	SD	MEAN	SD		
Glucose	Pyruvate	unlabelled	0,24	0,03	0,43	0,14	0,0197	3
		Labelled	0,76	0,03	1.12	0,14		
	Lactate	unlabelled	0,28	0,03	0,54	0,21	0,0017	3
		Labelled	0,72	0,03	1,36	0,21		
	Alanine	unlabelled	0,37	0,01	0,72	0,13	0,0007	3
		Labelled	0,63	0,01	1,20	0,13		
	Citrate	unlabelled	0,32	0,02	0,39	0,03	0,0846	3
		Labelled	0,68	0,02	0,65	0,03		
Glutamine	Glutamine	unlabelled	0,08	0,04	0,17	0,08	0,0040	3
		Labelled	0,92	0,04	1,64	0,08		
	Fumarate	unlabelled	0,47	0,05	0,48	0,08	0,4670	3
		Labelled	0,53	0,05	0,57	0,08		
	Citrate	m+4	1,00	0,02	0,90	0,01	0,0002	3
		m+5	1,00	0,04	1,16	0,06	0,0070	3

Table S3: List of primers used for vector construction and gene targeting

Genes	Forward primers sequence (5'-3')	Reverse primers sequence (5'-3')
m HK2	CCGTGGTGGACAAGATAAGAGAGAAC	GGACACGTCACATTTCGGAGCCAG
h HK2	TCCTCAGTAGAACATGGCAG	TGACATTAGCACTGGTGGAG
m LDHA	AGACAAACTCAAGGGCGAGA	GCGGTGATAATGACCAGCTT
m SLC2A1	AGGTCACCATCTTGGAGCTG	ACAGCGACACCACAGTGAAG
h SLC2A1	TTCACTGTCGTGTCGCTGTTT	AGCGCGATGGTCATGAGTAT
m VEGF	GGAGAGCAGAAGTCCCATGA	ACTCCAGGGCTTCATCGTTA
h VEGF	TACCTCCACCATGCAAAGTG	ATGATTCTGCCCTCCTCCTTC
m PPARGC1A	CAGTCCTTCCTCCATGCCTG	GGGTTTGTTCTGATCCTGTGG
h PPARGC1A	CCTGTGATGCTTTTGCTGCTCTTG	AAACTATCAAAATCCAGAGAGTCA
m PPARGC1B	CAGCCAGTACAGCCCCGATG	GGTGTGTCGCCTTCATCCAG
h PPARGC1B	GTACATTCAAAATCTCTCCAGCGACAT	GAGGGCTCGTTGCGCTTCCTCAGGGC
m ATP5J	GCGCGGAAGTAGAACGGT	GAGACTGCTGACCGAAGGAC
m COX7A	CAGTACACTTGAAAGGCGGG	CCAGCCCAAGCAGTATAAGC
m NDUFB5	TGGCAAGAGACTGTTTGTCG	AGCTGCGCTTCACCAATAAA
m TFAM	CGGCAGAGACGGTTAAAAA	GAATCATCCTTTGCCTCCTG
m NRF1	CTTACAAGGTGGGGGACAGA	ATGCTCACAGGGATCTGGAC
m NRF2	TGAGAAACTTAGCCGTGCATT	TGAGAAACTTAGCCGTGCATT
m RPLP0	GCAGCAGATCCGCATGTCGCTCCG	ACCAGACGGTTCAGTTCTGC
h RPLP0	GCAATGTTGCCAGTGTCTG	GCCTTGACCTTTTCAGCAA
h 18S rRNA	AACCCGTTGAACCCCATT	CCATCCAATCGGTAGTAGCG
h *cyt- b mtDNA	GCGTCCTTGCCCTATTACTATC	CTTACTGGTTGTCCTCCGATTC
h RPL13A nDNA	CTCAAGGTCGTGCGTCTG	TGGCTTTCTCTTTCCTCTTCTC
m COX2 mtDNA	GCCGACTAAATCAAGCAACA	CAATGGGCATAAAGCTATGG
m β globin nDNA	GAAGCGATTCTAGGGAGCAG	GGAGCAGCGATTCTGAGYAGA
m Flcn S62A	CGGGTCCGTGCCCACGCTCCAGCCGAG GGTGCCAGC	GCTGGCACCCTCGGCTGGAGCGTGGG C ACGGACCCG

* cyt-b: cytochrome b

Supplemental references:

1. Welbourn S, Green R, Gamache I, Dandache S, Lohmann V, Bartenschlager R, Meerovitch K, and Pause A. Hepatitis C virus NS2/3 processing is required for NS3 stability and viral RNA replication. *J Biol Chem.* 2005;280(33):29604-11.
2. Xu J. Preparation, culture, and immortalization of mouse embryonic fibroblasts. *Curr Protoc Mol Biol.* 2005;Chapter 28(Unit 28 1.
3. Faubert B, Boily G, Izreig S, Griss T, Samborska B, Dong Z, Dupuy F, Chambers C, Fuerth BJ, Viollet B, et al. AMPK is a negative regulator of the Warburg effect and suppresses tumor growth in vivo. *Cell Metab.* 2013;17(1):113-24.
4. Baba M, Hong SB, Sharma N, Warren MB, Nickerson ML, Iwamatsu A, Esposito D, Gillette WK, Hopkins RF, 3rd, Hartley JL, et al. Folliculin encoded by the BHD gene interacts with a binding protein, FNIP1, and AMPK, and is involved in AMPK and mTOR signaling. *Proc Natl Acad Sci U S A.* 2006;103(42):15552-7.
5. Lu X, Wei W, Fenton J, Nahorski MS, Rabai E, Reiman A, Seabra L, Nagy Z, Latif F, and Maher ER. Therapeutic targeting the loss of the birt-hogg-dube suppressor gene. *Mol Cancer Ther.* 2011;10(1):80-9.
6. Reiman A, Lu X, Seabra L, Boora U, Nahorski MS, Wei W, and Maher ER. Gene expression and protein array studies of folliculin-regulated pathways. *Anticancer Res.* 2012;32(11):4663-70.
7. MacIver NJ, Blagih J, Saucillo DC, Tonelli L, Griss T, Rathmell JC, and Jones RG. The liver kinase B1 is a central regulator of T cell development, activation, and metabolism. *J Immunol.* 2011;187(8):4187-98.
8. Preston RS, Philp A, Claessens T, Gijezen L, Dydensborg AB, Dunlop EA, Harper KT, Brinkhuizen T, Menko FH, Davies DM, et al. Absence of the Birt-Hogg-Dube gene product is associated with increased hypoxia-inducible factor transcriptional activity and a loss of metabolic flexibility. *Oncogene.* 2011;30(10):1159-73.

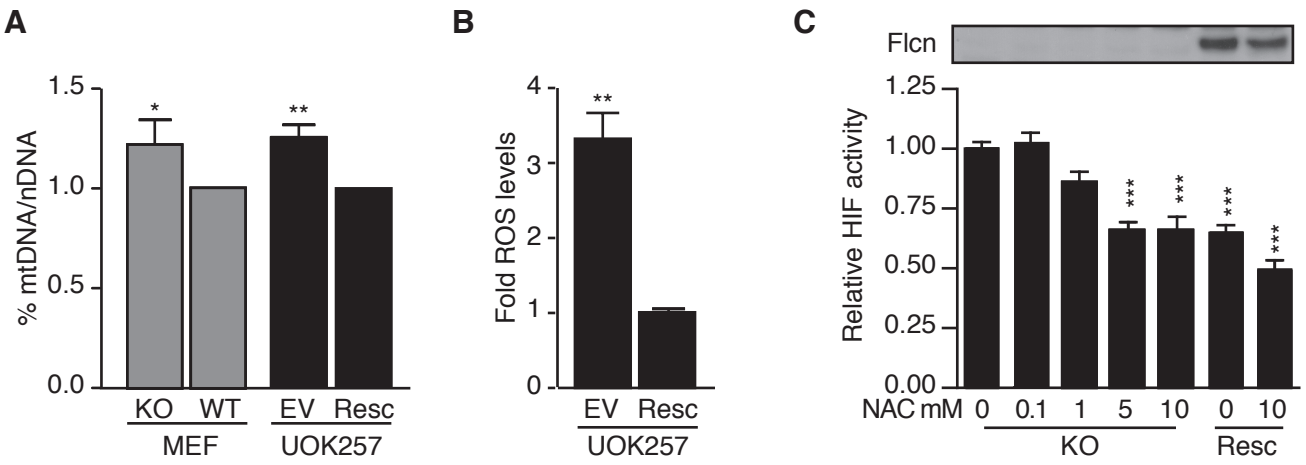

Supplementary Figure S1: Increase mitochondrial biogenesis in FLCN deficient human kidney cancer cells and ROS-dependent activation of HIF upon loss of FLCN in MEFs under hypoxia. A) Percent mitochondrial DNA content (mtDNA) normalized to nuclear DNA content (nDNA) measured in the indicated MEFs and the FLCN-deficient UOK257 (EV) and FLCN rescued (Resc) human kidney cancer cells. B) Fold ROS levels measured in the indicated UOK257 cells. C) Relative HIF activity measured under hypoxia using HIF-luciferase reporter assay in Flcn knockout MEFs, rescued (Resc) or not (KO) for FLCN expression and treated with the indicated concentrations of the anti-oxidant, N-acetyl cysteine (NAC) for 16 h. Data represent the means ± SD of 3 independent experiments performed in triplicate. *$p < 0.05$, **$p < 0.01$, ***$p < 0.001$.

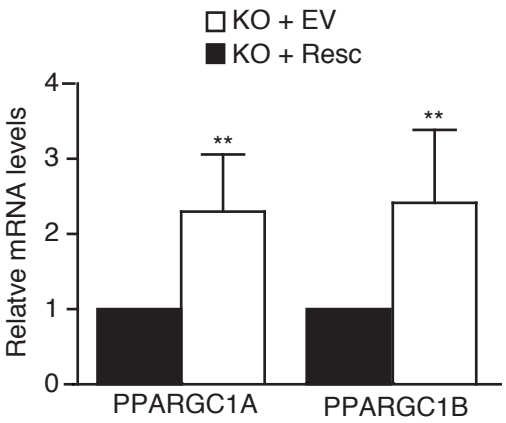

Supplementary Figure S2: PPPARCG1 upregulation upon loss of FLCN in human kidney cancer cells. Relative PPARGC1A and PPARGC1B mRNA expression levels measured in FLCN-deficient (EV) and FLCN rescued (WT) human kidney UOK257 cancer cells. Data represent the means ± SD of five independent experiments performed in triplicate. **$p < 0.01$.

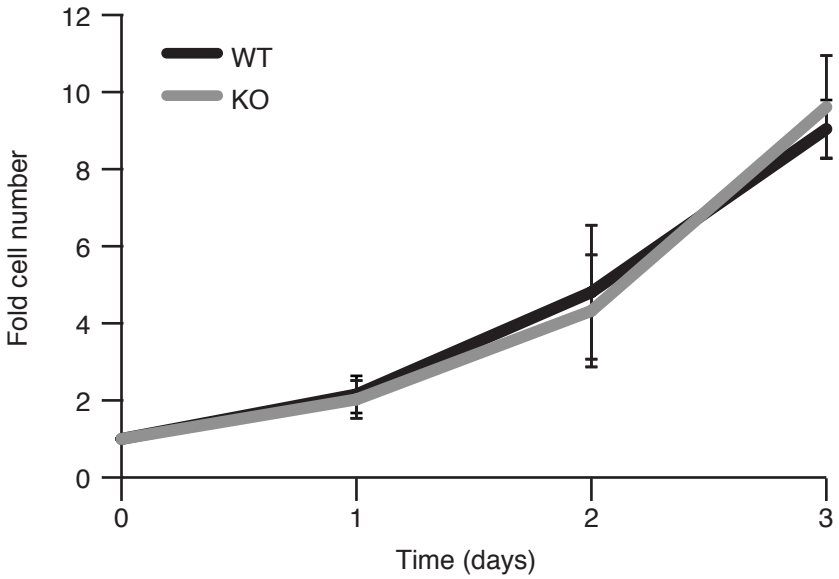

Supplementary Figure S3: Loss of FLCN in MEFs does not affect cell proliferation. *Flcn* WT and KO MEFs proliferation rate were determined by cell counting in time course experiments. Data represent the mean ± SD of six independent experiments performed in triplicate.

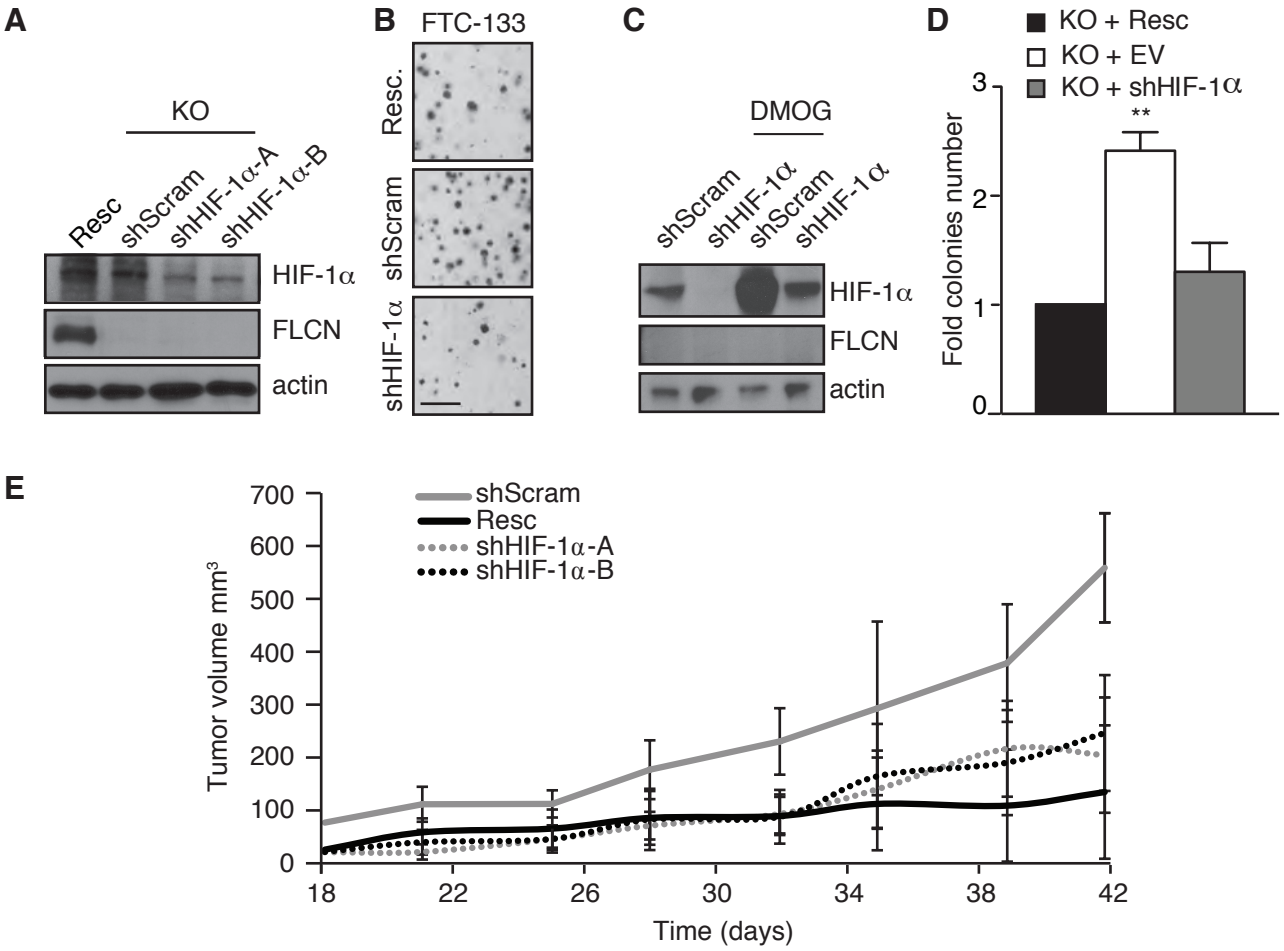

Supplementary Figure S4: HIF-dependent metabolic advantage drives tumorigenesis in FLCN null cancer cells. A, C) Western blot analysis of FLCN and HIF-1α expression levels in the indicated FTC-133 (A) and UOK257 (C) cancer cell lines. Actin was shown as loading control. When indicated, cells were pretreated with Dimethyloxaloylglycine (DMOG), an inhibitor of HIF-1α prolyl hydroxylases that prevent HIF-1α degradation. Results are representative of 3 independent experiments. B) Representative pictures of soft agar colonies in the indicated FTC-133 cell lines. Scale bar: 500μM. D) Quantification of soft agar colonies number relative to FLCN-deficient UOK257 cells rescued for FLCN expression (KO + Resc). Data represent the means ± SD of 4 independent experiments performed in triplicate. E) Time course measurement of xenograft tumor volume in the indicated FTC-133 cell lines. n= 5 mice per group.